

# Conditional Kernel Density Estimation Considering Autocorrelation for Renewable Energy Probabilistic Modeling

Yuchen SHI and Nan CHEN

Department of Industrial Systems Engineering and Management  
National University of Singapore  
Singapore

## Abstract

Renewable energy is essential for energy security and global warming mitigation. However, power generation from renewable energy sources is uncertain due to volatile weather conditions and complex equipment operations. To improve equipment's operation efficiency, it is important to understand and characterize the uncertainty in renewable power generation. In this paper, we proposed a conditional kernel density estimation method to model the distribution of equipment's power output given any weather conditions. It explicitly accounts for the temporal dependence in the data stream and uses an iterative procedure to reduce the bias in kernel density estimation. Compared with existing literature, our approach is especially useful for the purposes of equipment condition monitoring or short-term renewable energy forecasting, where the data dependence plays a more significant role. We demonstrate our method and compare it with alternatives through real applications.

*Keywords:* Renewable energy; Kernel; Conditional Density Estimation; Temporal dependence.

## 1 Introduction

### 1.1 Background and Research Problem

With technologies getting maturer and cheaper, renewable energy (RE) plays a more and more essential role in enhancing energy security and mitigating global warming. As reported by Renewable Energy Policy Network for the 21st Century (REN21), the global renewable

capacity reached 2378 GW by the end of 2018 and is estimated to provide more than 26% of global electricity generation (Bacher et al., 2009). Moreover, renewable energy sources (RES) and electrification have the potential to provide 75% of the necessary reductions in energy-related carbon emissions to limit the global rise in temperature by 2050 (IRENA, 2019). Nevertheless, one major challenge caused by increasing RE penetration in the energy portfolio is the fluctuating power generation, as shown in the middle and right panel of Figure 1, which requires advanced system balancing of supply and demand. Such fluctuations are seen more often for power generated from variable renewable energy (VRE), i.e., renewable energy that is not stored prior to power generation. The dominant VRE technologies are wind and solar energy, whereas run-of-the-river hydroelectricity, namely tidal energy and wave energy are also included (Cochran et al., 2012). Among VRE, wind and solar energy are especially important. Their shares of energy portfolio are expected to substantially increase from 7% and 3% of current state to 35% and 25% by 2050, respectively (IRENA, 2019). This leads to the essential topic of understanding and characterizing uncertainty in RES.

Generally speaking, the uncertainties contained in typical RES are two-fold. Firstly, the weather conditions are uncertain. RES are usually harvested from natural processes, such as sunlight, wind, rain, tides, waves, and geothermal heat. Due to this nature, forecasting weather conditions plays a crucial rule in RE forecasting. Yet forecasting weather condition is a relatively independent topic and not the focus of this work. Interested readers can refer to Lei et al. (2009); Bacher et al. (2009); Zhang et al. (2017) and references therein. Secondly, the functional relationships between power production and various weather conditions are unclear, due to complex system operations. In other words, even if accurate weather conditions can be obtained, the amount of power generated is still uncertain. We adopt the term “power curve” to refer to the relationship power generation and different weather conditions in this work. The term “power curve” is historically widely used to refer to the relation between wind power generated and wind speeds (Lee et al., 2015). Specifically, in this work, we

define “power curve” as the probabilistic modeling of renewable energy production under different weather conditions, which focuses on quantifying the uncertainty lies in the functional relationship. Given the definition of power curve, estimating power curve for uncertainty quantification is the main focus of this work. The importance and indispensability of power curve estimation have been pointed out for several impact areas for RES. Firstly, should power curve be combined with prediction of weather conditions, power curve can be used for RE forecasting (Hong et al., 2016). Accurate short-term RE forecasting is essential to improve system control (Aho et al., 2012), the security and efficiency of power grid (Blonbou, 2011), and power pricing and trading (Pinson et al., 2007). Moreover, power curve serves as a system performance modeling which is critical for condition monitoring and anomaly detection (Sohoni et al., 2016).

Estimating the power curve is inherently challenging because the mechanisms to harvest RE are usually complex, with an ambiguous rate of transfer of the energy. Taking wind power as an example, power generation of a wind turbine is a function of several parameters: radius of the rotor, air density and wind speed. Nevertheless, their relation does not follow a known functional form and depends on turbine type, blade pitch, tip-speed ratio, etc (Ackermann, 2005). Since blade pitch and tip-speed ratio are affected by turbines’ exposed weather conditions in an ambiguous way, modeling the power curve based on first principles is inaccurate. As a result, researchers have adopted statistical regression and data-driven methods for power curve modeling. Generally, modeling power curve has three challenges: (1) The system inputs, i.e., weather conditions, are highly interactive. As an example, the interaction between wind speed and wind direction on wind power production is shown in the left panel of Figure 1. (2) The conditional distributions of power production under different weather condition are heterogeneous. Consider the power production under a certain weather condition as a random variable, its conditional distribution has different mean, variances, even different distributional forms (Yuan et al., 2017), as shown in the middle and right panel of Figure 1. These two challenges make the conventional parametric regression less appealing.

Instead, nonparametric methods can deal with ambiguous interactions among weather conditions without distributional assumptions. Specifically, nonparametric conditional density estimation methods are appealing for the heterogeneous conditional distributions. Therefore, we use conditional density estimation for power curve modeling to quantify the uncertainty.

(3) There exists indispensable short-term temporal dependence in the data stream. This is possibly because of equipment’s inertia when it does internal controls in responding to weather conditions. Without properly accounting for data dependence, the inference could be less accurate or even misleading.

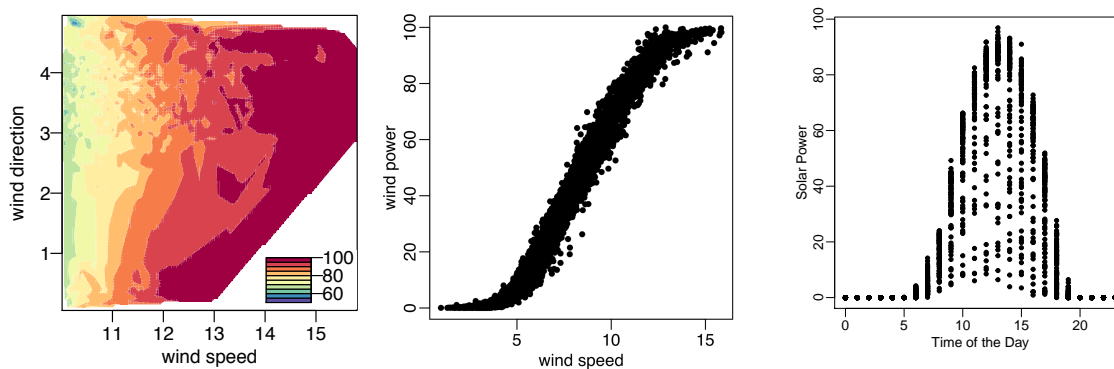


**Figure 1:** Left figure: heat map of wind power production at different wind speeds and directions. Middle panel: scatter plot of wind power production versus wind speed (using 10-min average records). Right panel: scatter plot of solar power production versus time of the day (using hourly average records)

The first and second challenges have been addressed in the literature. Compared with the existing method, in this paper, we explicitly account for the short-term temporal dependence, i.e., third challenge of modeling power curve. Our proposed method model the conditional power output distribution in a nonparametric way that is able to account for the temporal dependence and improves the inference efficiency and forecasting accuracy.

## 1.2 Literature Review

Overall, literature on power curve estimation can be classified into two categories: conditional mean estimation and conditional density estimation. Methods in the first category focus on the conditional mean of power production ( $Y$ ) at given weather condition ( $\mathbf{X}$ ),

i.e.,  $\mathbb{E}(Y|\mathbf{X})$ . Within this category, [Lave et al. \(2012\)](#) proposed a wavelet variability model for solar power using solar irradiance and spatial-temporal correlation. [Lydia et al. \(2014\)](#) provided reviews on the methods for wind power curve estimation. Their review include typical parametric and nonparametric methods such as copula, spline interpolation, and fuzzy models. With additional parametric distributional assumption, conditional mean estimation can also provide probabilistic forecasting. For example, [Pinson et al. \(2012\)](#) realized probabilistic forecasting of wave energy through a log-normal density assumption. This category manages to consider the effects of weather conditions and their interactions on average power production, yet fails to capture the heterogeneous conditional distribution of power output.

To capture the heterogeneous conditional distribution, methods in the second category provide conditional density  $f(Y|\mathbf{X})$  at input  $(\mathbf{X})$ . Within this category, wind energy is one of the sub-domains that has relatively higher research maturity ([Hong et al., 2016](#)). [Jeon and Taylor \(2012\)](#) dealt with the inherent uncertainty in weather conditions using VARMA-GARCH (vector autoregressive moving average-generalized autoregressive conditional heteroscedastic) and adopted conditional kernel density for wind power forecasting at individual wind farms. [Lee et al. \(2015\)](#) further analyzed the functional relationship between wind power and various weather conditions. They proposed an additive nonparametric model to include as many weather conditions as possible to improve the relationship modelling. Besides wind energy, conditional density estimations have also been shown to be promising for other RES, such as wave energy and solar energy. Recently, [Jeon and Taylor \(2016\)](#) constructed the kernel density of wave energy conditional on wind speed. [Golestaneh et al. \(2016\)](#) designed the extreme learning method to generate predictive densities using extra criteria and formulas. Overall, conditional density estimation requires minimal distributional assumptions and manages to make flexible distributional inference. Most of the literature discussed above assumed that the power production data are independent. However, in a short time period, dependency between neighboring observations cannot be neglected. To the best of our knowledge, although there exist a rich amount of works that consider

short-term temporal dependence, no work reported incorporates temporal dependence with conditional density nonparametrically. The existed works focus on the conditional mean of power production and the uncertainties can be quantified with parametric assumptions, such as the Gaussian assumption. In this category, some works focus on power production time series only. [Pinson and Madsen \(2012\)](#) used Markov switching autoregressive (MSAR) to model different regimes in wind power production. [Fusco and Ringwood \(2010\)](#) considered the wave energy as a univariate time series and constructed a series of models including cyclical model, extended Kalman filter, AR models and neural networks. Some other works also consider weather conditions as explanatory variables. [Sanchez \(2006\)](#) proposed short-term wind power forecasting method as a combination of several AR and ARX models, which included multi-period-ahead autoregressions considering wind speed, wind direction, lagged wind power and daily cycles as regressors. [Lauret et al. \(2015\)](#) proposed several benchmarking supervised learning methods for solar radiance forecasting, which included neural networks, support vector machine, simple linear autoregressive model as well as persistent based methods. Based on the listed literature, a natural research gap is to account for the temporal dependence when modelling the conditional power output distribution, i.e., to consider temporal dependence for conditional density estimation, thus improving the inference and prediction efficiency.

### 1.3 Contribution and Outlines

This paper proposes a novel conditional density estimation method for RE. It accounts for the temporal dependence in the observations and reduce the bias due to unconstant mean function. We first account for the autocorrelated error in the conditional mean. The conditional density is established afterwards. We name the method conditional kernel Density Estimation considering AutocoRrelation (DEAR) for convenience.

The remainder of this paper is organized as follows. In Section 2, we review the conventional kernel method. In Section 3, we introduce our proposed method. In Section 4,

we demonstrate the effectiveness of our proposed method by case studies. In Section 5, we conclude the paper with discussions.

## 2 A Review of Conventional Kernel Method

In this section, we briefly review the conventional kernel method and discuss its limitation. The idea of kernel density estimation can be traced back to Rosenblatt (1969). Suppose we have  $N$  observations  $\{\mathbf{X}_i, Y_i\}$ ,  $i = 1 \cdots N$ , where  $\mathbf{X}_i \in \mathbb{R}^d$  is a vector of input variables and  $Y_i \in \mathbb{R}$  denotes the corresponding output value. Let  $\hat{f}_{\mathcal{K}}$  denote the conventional conditional kernel density estimator:

$$\hat{f}_c(Y|\mathbf{X}) = \sum_{i=1}^N w_i(\mathbf{X})\mathcal{K}(Y - Y_i; h_y), \quad (1)$$

where

$$w_i(\mathbf{X}) = \frac{\mathcal{K}(\|\mathbf{X} - \mathbf{X}_i\|; \mathbf{h}_{\mathbf{X}})}{\sum_{i=1}^N \mathcal{K}(\|\mathbf{X} - \mathbf{X}_i\|; \mathbf{h}_{\mathbf{X}})}. \quad (2)$$

Here,  $\mathcal{K}(\cdot; h)$  is the kernel function, which is assumed to be a real-valued, integrable and non-negative symmetric function.  $\mathbf{h}_{\mathbf{X}}$  and  $h_y$  denote the smoothing parameter (bandwidth) to be chosen adaptively. They are crucial parameters that control the performance of estimation. A larger bandwidth makes the kernel estimator smoother, but increases the bias. A smaller bandwidth does the opposite. Based on (1), we can obtain the conditional mean estimator by integration:

$$\hat{\mathbb{E}}_c(Y|\mathbf{X}) = \int y\hat{f}(y|\mathbf{X})dy = \sum_{i=1}^N w_i(\mathbf{X})Y_i, \quad (3)$$

Throughout the paper, the method above is referred to as the *conventional kernel method*. Despite its simplicity, conventional kernel estimators have some limitations. Firstly, when the conditional mean is not constant, conventional kernel estimation can be biased because of possible asymmetry effect, curvature effect, or boundary effect in the data. Figure 2 shows an example of bias caused by asymmetry effect. There are more samples on the right-hand

side of  $x_0$  than left. When the conditional mean is constant, there is no estimation bias, as in the left panel. However, in RE applications, the asymmetric samples cause a biased conditional mean estimation, i.e.,  $\hat{\mathbb{E}}(y|x_0) > y_0$ . Similarly, conditional density estimation becomes biased as well. Besides the cause of asymmetry, bias is introduced when  $x_0$  is near domain boundary or when the mean function has severe curvature. Further details have been explained in [Hastie and Loader \(1993\)](#).

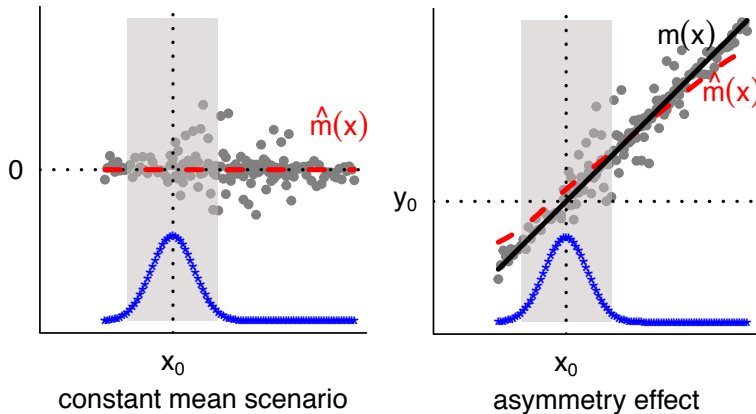


**Figure 2: The bias of conventional kernel caused by asymmetry effects.** The solid (black) curve is the real function, the dashed (red) curve is the estimated conditional mean function by conventional kernel. The dotted (blue) curve is the weights of reference points assigned by a kernel.

In addition, conventional kernel estimation assumes data are independent. It does not consider temporal dependence. However, in RE data streams, autocorrelation among data is common. To demonstrate the autocorrelation, we fit the conditional mean of wind power and compute the residuals. The conditional mean is estimated using Additive Multiplicative Kernel (AMK) ([Lee et al., 2015](#)) as an example, which is the state-of-art method for wind power curve modeling in the literature. [Figure 3](#) shows the autocorrelation function (ACF) of residuals and a segment of consecutive residuals. The ACF plot and residual series indicate possibly strong temporal dependence in the wind power data.

Last but not least, conventional kernel method suffers from “curse of dimensionality”, even if the input dimension of  $\mathbf{X}$  is as high as 4 or 5. The essence of kernel trick is to use samples who have similar inputs as references for inference. Given the definition in (2),  $w_i$  should asymptotically place dominant mass in a convex region centered at  $\mathbf{X}$ , controlled by



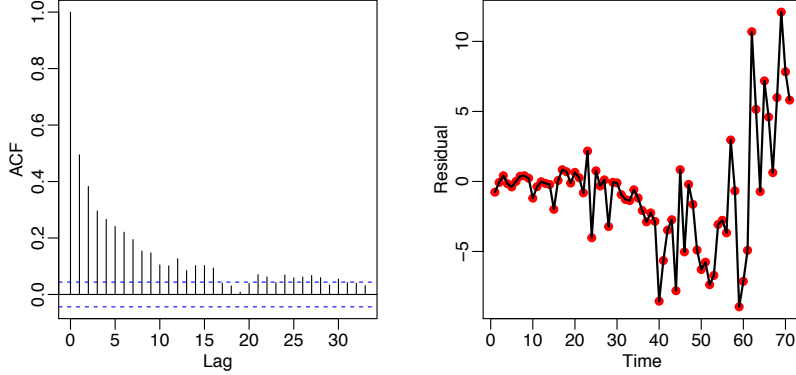


**Figure 3:** Temporal dependence in wind power data of dataset 1 in Section 4; Left panel: The ACF plot; Right panel: a sample of consecutive residuals.

the smoothing parameter  $h_{\mathbf{X}}$ . As the dimension  $d$  increases, the probability of having enough sample in a unit area in the  $d$ -dimensional space diminishes exponentially. There were some attempts to tackle this difficulty. For example, Lee et al. (2015) introduced an additive structure on the conventional kernel methods. The kernel used in Lee et al. (2015) is an addition of several kernels with at most three dimensional inputs. To improve the conditional density estimation for power curve, our new method considers the bias from non-constant mean and data autocorrelation effectively. At the same time, it adopts an additive structure proposed by Lee et al. (2015) when necessary to avoid “curse of dimensionality”.

### 3 Conditional Kernel Density Estimation Considering Autocorrelation (DEAR)

In this section, we introduce our proposed method and explain the inference procedure. Henceafter, we name the proposed method as *conditional kernel Density Estimation considering AutocoRrelation* (DEAR). Let  $\mathcal{F}_T$  denote the set that contains all historical data up to time  $T$ ,  $\mathcal{F}_T := \{(\mathbf{X}_t, Y_t), t = 1, \dots, T\}$ , where  $\mathbf{X}_t \in \mathbb{R}^d$  and  $Y_t \in \mathbb{R}$ . Assume the data follows the model:

$$Y_t = m(\mathbf{X}_t) + \sigma(\mathbf{X}_t)u_t, \tag{4}$$

where  $m(\cdot)$  and  $\sigma(\cdot)$  are unknown smooth functions denoting conditional mean and conditional standard deviation.  $u_t$  is a stationary process with mean 0.  $u_t$  can be expressed in the autoregressive representation with order  $p$ :

$$u_t = \sum_{\tau=1}^p a_\tau u_{t-\tau} + \epsilon_t, \quad (5)$$

where  $\epsilon_t$  are independently and identically distributed (*i.i.d.*) with mean zero and follow unknown distribution.  $p$  can be chosen to be suitably small relative to the sample size  $T$  and determined adaptively by data. Following this model, the conditional mean can be expressed as

$$\mu_{t|t-1} := \mathbb{E}(Y_t | \mathbf{X}_t, \mathcal{F}_{t-1}) = m(\mathbf{X}_t) + \sigma(\mathbf{X}_t) \sum_{\tau=1}^p a_\tau [Y_{t-\tau} - m(\mathbf{X}_{t-\tau})] / \sigma(\mathbf{X}_{t-\tau}). \quad (6)$$

Since  $\mu_{t|t-1}$  is a constant, the following equality for the conditional density of  $Y$  holds:

$$f(Y_t | \mathbf{X}_t, \mathcal{F}_{t-1}) = \sigma(\mathbf{X}_t) g[(Y_t - \mu_{t|t-1}) / \sigma(\mathbf{X}_t)], \quad (7)$$

$$= \sigma(\mathbf{X}_t) g(\epsilon_t) \quad (8)$$

Here  $f$  stands for the conditional density function of  $Y$  and  $g$  stands for the density function of  $\epsilon$ . (7) is established based on the assumption that  $\epsilon_t$  are *i.i.d.* According to (7),  $\sigma(\mathbf{X}_t)\epsilon_t$  has the same distribution as  $Y_t$  except for a shift on the conditional mean (Hyndman et al., 1996). In other words, estimating the conditional density of  $Y_t$  equals to estimating  $\sigma(\mathbf{X}_t)g(\epsilon_t)$ . Equation (6)-(7) shows the essential difference between our proposed method and conventional kernel method. In our proposed model, an autocorrelation process is firstly imposed on conditional mean. Conditional density is then built on the residual of conditional mean, which is expected to be uncorrelated.

### 3.1 Inference Procedure of DEAR

We first discuss the inference procedure for DEAR’s conditional mean function. The conditional mean of power curve is usually not constant. Given DEAR’s model structure, we now have the flexibility to apply higher order local regression for  $m(\cdot)$ , such as local linear regression or local polynomial regression, to reduce the bias caused by conventional kernel methods. In our case studies,  $\tilde{m}(\cdot)$  is estimated by local linear regression. Details of local linear regression are provided in the supplementary file. From our experience, local linear regression can effectively reduce the bias and is sufficient for power curve estimation. Higher order local polynomial regressions causes more severe “curse of dimensionality”. In the following, we represent the initial conditional mean estimator as  $\tilde{m}(\cdot)$ , which is estimated using dataset  $\mathcal{F}_T$ . Similarly,  $\sigma(\cdot)$  can be estimated with flexible choice through the residual of conditional mean estimator. When data are independent, we have squared residuals defined as

$$Z_t := [Y_t - \tilde{m}(\mathbf{X}_t)]^2 \quad \text{for } t = 1, \dots, T. \quad (9)$$

The conditional variance estimator is then represented as  $\tilde{\sigma}^2(\cdot)$ , which can be estimated by the dataset  $\mathcal{G}_T := \{(\mathbf{X}_t, Z_t), t = 1, \dots, T\}$ .

$\tilde{m}(\cdot)$  and  $\tilde{\sigma}(\cdot)$  are standard estimators when data are independent. However, they can be less efficient when data are temporal dependent. In order to account for the autocorrelation, we use an iterative procedure to estimate the  $m(\cdot)$ ,  $\sigma(\cdot)$ , and parameters  $a_\tau$ . The iterative procedure takes  $\tilde{m}(\cdot)$  and  $\tilde{\sigma}(\cdot)$  as the initial estimates of the mean function and standard deviation function. Given these estimation, we further estimate the AR parameters. The estimated AR parameters in return can update the  $\hat{m}(\cdot)$  and  $\hat{\sigma}(\cdot)$ . We summarize the two-step iterative procedure as follows.

**Step 1: Estimate AR parameters given  $\hat{m}(\cdot)$  and  $\hat{\sigma}(\cdot)$**

Given existing estimates  $\hat{m}(\mathbf{X})$  and  $\hat{\sigma}(\mathbf{X})$  of the mean function and standard deviation function, it is straightforward to estimate the parameters  $\{a_1, \dots, a_p\}$  associated with the

autoregressive process  $u_t$ . According to the model (4) and (5), we can transform the observation sequence  $Y_t$  to  $u_t$  by  $\tilde{u}_t = \hat{\sigma}(\mathbf{X}_t)^{-1}[Y_t - \hat{m}(\mathbf{X}_t)]$  for  $t = 1, \dots, T$ .  $\tilde{u}_t$  is a stationary process when  $\hat{m}(\mathbf{X})$  and  $\hat{\sigma}(\mathbf{X})$  are consistently estimated. Its autoregressive parameters can be estimated using conventional time series techniques. To account for flexible distribution of  $\epsilon_t$ , we choose the least square approach

$$\hat{a}_1, \dots, \hat{a}_p = \arg \min_{a_1, \dots, a_p} \sum_{i=p+1}^T [\tilde{u}_i - a_1 \tilde{u}_{i-1} - \dots - a_p \tilde{u}_{i-p}]^2 \quad (10)$$

**Step 2: Update  $\hat{m}(\cdot)$  and  $\hat{\sigma}(\cdot)$  given AR parameters**

Given the estimated AR parameters in Step 1 and previous estimates  $\hat{m}(\mathbf{X})$  and  $\hat{\sigma}(\mathbf{X})$ , we are able to improve the estimation of the mean function and standard deviation function. According to (4),  $m(\mathbf{X}_t) = Y_t - \sigma(\mathbf{X}_t) \sum_{\tau=1}^p a_\tau u_{t-\tau}$ . We define

$$\tilde{Y}_t = Y_t - \hat{\sigma}(\mathbf{X}_t) \sum_{\tau=1}^p \hat{a}_\tau \tilde{u}_{t-\tau}. \quad (11)$$

Because of the autocorrelation, it can be shown that  $\mathbb{E}(\tilde{Y}_t)$  is closer to  $m(\mathbf{X}_t)$  than  $\mathbb{E}(Y_t)$ . As a result, substituting  $Y_t$  by  $\tilde{Y}_t$  yields a more accurate estimator. Likewise,  $\hat{\sigma}(\mathbf{X})$  can be correspondingly updated using  $\tilde{Z}_t = \log[\tilde{Y}_t - \hat{m}(\mathbf{X}_t)]^2$  instead of  $Z_t$  in (9).

In the next iteration, the latest estimation  $\hat{m}(\cdot)$  and  $\hat{\sigma}(\cdot)$  can update the stationary process  $\tilde{u}_t$ , and hence the AR parameters. A few iterations may be sufficient to improve performance with finite samples in practice. It can be proved that under mild conditions,  $\hat{m}(\mathbf{X}_t)$  estimated by this iterative procedure has the same asymptotic bias as the estimator  $\tilde{m}(\mathbf{X}_t)$  for *i.i.d* errors. But  $\hat{m}(\mathbf{X}_t)$  has smaller variance than  $\tilde{m}(\mathbf{X}_t)$  because autocorrelations are taken into account, which makes it more efficient (Xiao et al., 2003).

After the iterations terminate, we can obtain the conditional mean estimator as

$$\hat{\mu}_{t|t-1} = \hat{m}(\mathbf{X}_t) + \hat{\sigma}(\mathbf{X}_t) \sum_{\tau=1}^p \hat{a}_\tau \hat{u}_{t-\tau}. \quad (12)$$

Here  $\hat{u}_t = \hat{\sigma}(\mathbf{X}_t)^{-1}[Y_t - \hat{m}(\mathbf{X}_t)]$ . To estimate the conditional density of  $Y_t$ , it is suffice to estimate the density of  $\epsilon_t$ , with a scale transformation. Since the error term  $\epsilon_t$  are independent and identically distributed with mean zero, conventional kernel estimator of (1) can be used. To be more specific, given  $\hat{\mu}_{t|t-1}$  in equation (12), the homoscedastic residual can be defined using the one step ahead forecasting residuals as  $r_t := (Y_t - \hat{\mu}_{t|t-1})/\hat{\sigma}(\mathbf{X}_t)$ . Therefore, we have the conventional kernel density estimate of  $r_t$  as:

$$\hat{g}(r_t) = \frac{1}{T} \sum_{i=1}^T \mathcal{K}(r_t - r_i; h_r), \quad (13)$$

By equation (7), the conditional density of  $Y$  can be estimated by:

$$\hat{f}(Y_t|\mathbf{X}_t, \mathcal{F}_{t-1}) = \frac{1}{T} \sum_{i=1}^T \mathcal{K}(Y_t - \hat{\mu}_{t|t-1} - r_i \hat{\sigma}(\mathbf{X}_t); \hat{h}_r \hat{\sigma}(\mathbf{X}_t)). \quad (14)$$

In the end, for a new input point  $\mathbf{X}_{T+1}$ , we have the conditional mean predictor:

$$\hat{\mu}_{T+1|T} = \hat{m}(\mathbf{X}_{T+1}) + \hat{\sigma}(\mathbf{X}_{T+1}) \sum_{\tau=1}^p \hat{a}_\tau \hat{u}_{T+1-\tau}, \quad (15)$$

and the conditional density for  $Y_{T+1}$  as:

$$\hat{f}(Y_{T+1}|\mathbf{X}_{T+1}, \mathcal{F}_T) = \frac{1}{T} \sum_{i=1}^T \mathcal{K}(Y_{T+1} - \hat{\mu}_{T+1|T} - r_i \hat{\sigma}(\mathbf{X}_{T+1}); h_r \hat{\sigma}(\mathbf{X}_{T+1})). \quad (16)$$

## 3.2 Further Discussion on Implementation

### 3.2.1 Choice of Kernel

For the choice of kernel, we mainly follow the setting in Lee et al. (2015). For each non-circular univariate variable, we use the Gaussian kernel:

$$\mathcal{K}(u; h) = (1/\sqrt{2\pi}h) \cdot \exp[-u^2/(2h^2)]. \quad (17)$$

Here  $u$  is the euclidean distance between two points of interest, and  $h$  is the bandwidth. For circular variables, such as wind direction, special treatment is needed because 0 degrees and 360 degrees are identical. We use Von Mises kernel, which is known as the circular normal distribution:

$$\mathcal{K}(u; h) = \exp[h^{-2} \cos(u)] / (2\pi I_0(h^{-2})). \quad (18)$$

Here  $I_0(\cdot)$  is the modified Bessel function of order 0,  $1/h^2$  is the concentration parameter, as recommended by [Taylor \(2008\)](#).

When dealing with multivariate variables, we choose the multiplicative kernel, i.e., a multiplication of univariate kernel functions, as the base kernel. To be more specific,

$$\mathcal{K}(\|\mathbf{X} - \mathbf{X}_i\|; \mathbf{h}_{\mathbf{X}}) := \prod_{j=1}^d \mathcal{K}(X_j - X_{i,j}; h_j) \quad (19)$$

where  $\mathcal{K}(\cdot; h_j)$ ,  $j = 1, \dots, d$  are univariate kernels. Kernel based methods faces “curse of dimensionality” when the input dimension goes higher. We adopt the idea of [Lee et al. \(2015\)](#) and use an additive structure on the multiplicative kernels when there are more than three variables considered. To be more specific, we limit each multiplicative kernel to be product kernels of at most three inputs and build an additive model of all the multivariate kernels. This additive structure has been shown effective in alleviating the “curse of dimensionality”.

### 3.2.2 Choice of Bandwidth

Bandwidth is a key parameter for kernel performance. In this work, we choose heuristic bandwidth selectors as follows.

Firstly, we use the direct plug-in methods to determine bandwidths for every variable separately. Direct plug-in kind of methods choose bandwidths by minimizing the mean integrated square error (MISE) or its asymptotic approximation. For mean function  $\tilde{m}_j(\cdot) =$

$\mathbb{E}[Y|X_j]$ , its MISE for  $j = 1, 2, \dots, d$  is (Ruppert et al., 1995)

$$\text{MISE} \{ \tilde{m}_j(x; h_j) \} = \mathbb{E} \left[ \int \{ \tilde{m}_j(x; h_j) - m_j(x) \}^2 f_j(x) dx \right], \quad (20)$$

In our application, we use local linear regression to obtain  $\tilde{m}(\cdot)$ , in which case the direct plug-in bandwidths can be obtained following the methods proposed by Ruppert et al. (1995). For the conditional standard deviation function, the bandwidths for  $\sigma(\cdot)$  are chosen similarly to that for  $m(\cdot)$ .

On the other hand, the MISE for density estimation of residual can be written as (Sheather and Jones, 1991):

$$\text{MISE} \{ \tilde{g}(r; h_r) \} = \mathbb{E} \int [\tilde{g}(r; h_r) - g(r)]^2 dr. \quad (21)$$

Based on (21),  $h_r$  is estimated by the direct plug-in method proposed by Sheather and Jones (1991). Details on the bandwidths selection are included in the supplementary file.

To further improve the estimation performance, we choose the adaptive bandwidth for the conditional density estimation. The adaptive approach allows the bandwidth of kernels to vary from one observation to another. Adaptive bandwidth provides a calibration for the individual bandwidths and improves estimation accuracy at the tail of the densities where the data becomes sparser. Both features can help to improve conditional density estimation especially with multivariate input variables. Following Silverman (1986), the adaptive bandwidth can be calculated as  $h_{r,i} = h_r \{ \bar{g}(r_i | \mathbf{X}_i) / s \}^{-1/2}$ , where  $s = \exp[n^{-1} \sum_{i=1}^T \log \bar{g}(r_i | \mathbf{X}_i)]$ , and  $\bar{g}(\cdot)$  is the conditional density function estimated using bandwidth  $h_r$  from (21).

We have compared our bandwidth selectors with multivariate plug-in bandwidth (Wand and Jones, 1994) and cross validation. The result shows that our bandwidth performs better than multivariate plug-in bandwidth and computes much faster than cross validation with comparable accuracy.

### 3.2.3 Implementation

There are several implementation details that worth further explanation. Firstly, in practice, the RE equipment makes internal adjustments to control the power output in a reasonable region. As a result, we set the upper and lower limits on the predicted values to make them sensible. Secondly, data sparsity causes poor performance for local linear regression. The sparsity can be determined by thresholding on the input density (Taylor and Einbeck, 2013). When data are sparse, we use conventional kernel to estimate the conditional mean. Thirdly, in a long time span, the power curve can change due to equipment’s degradation and maintenance. To update the power curve, we adopt a rolling window approach. Based on the above explanations, the detailed procedure for DEAR is summarized in Algorithm 1, which is provided in the supplementary file.

## 4 Case Studies

Two case studies are conducted to demonstrate the effectiveness of DEAR. We compare DEAR with a series of existing methods in the literature. For conditional density estimator, we choose additive multiplicative kernel (AMK) (Lee et al., 2015). For conditional mean estimator, we compare DEAR with the initial estimate of conditional mean ( $\tilde{m}(\cdot)$ ), i.e., additive multiplicative local linear regression (AML). Besides, we also compare DEAR with binning method since AMK is not designed for short-term purposes. Binning is the current industrial practice of estimating wind power curve Ding et al. (2015). Binning method discretizes the domain of every input variable into a finite number of bins. Statistics are then estimated within each bin. To compare with models considering temporal dependence, we choose Markov switching autoregression (MSAR) (Pinson and Madsen, 2012), which considers the response variable as an autoregressive process governed by the regime sequences. Besides, it is well known that persistent model is hard to outperform for short lead times (Ma et al., 2011), we also include persistent model for comparison. Last but not least, to



emphasize DEAR’s effectiveness on accounting for short-term temporal dependence, we compare DEAR with Kernel Density with Exponential Smoothing (KDES) (Bessa et al., 2012): a kernel with forgetting factor to adapt to the changes over time. Since DEAR uses a rolling window for the kernel estimation, we also update all the above method by using the most recent observation at each time step. In all our case studies, we use RMSE as the criteria to choose input variables for the local regression estimator  $\tilde{m}(\cdot)$ , DEAR and KDES choose the same input variable combinations as  $\tilde{m}(\cdot)$ .

Performance is evaluated by two criteria. For conditional mean estimation, we use root mean square error (RMSE) between observation and the estimated conditional mean:

$$\text{RMSE} = \sqrt{\frac{1}{N'} \sum_{t=1}^{N'} (\hat{\mu}_{t|t-1} - Y_t)^2},$$

where  $N'$  is the size of testing dataset. For conditional density estimation, we use the mean continuous ranked probability score (CRPS):

$$\text{CRPS} = \frac{1}{N'} \sum_{t=1}^{N'} \int (\hat{F}(y|\mathbf{X}_t, \mathcal{F}_{t-1}) - \mathbb{1}(y > Y_t))^2 dy,$$

where  $\hat{F}(y|\mathbf{X}_t, \mathcal{F}_{t-1})$  is the estimated conditional CDF and  $\mathbb{1}(\cdot)$  is the indicator function. CRPS measures the difference between the induced marginal distribution of  $Y$  and the empirical cumulative distribution. If the conditional density function is accurate, the discrepancy would be small.

## 4.1 Case 1: Wind Power Curve Estimation

This case study dataset is from the wind farm La Haute Borne (Meuse, France), provided by ENGIE Renewable Energy<sup>1</sup>. The dataset contains 10-min average historical data of 4 wind turbines (R80790, R80736, R80721, R80711) since 2013. Available weather conditions

---

<sup>1</sup>The dataset is available at <https://opendata-renewables.engie.com/pages/home/>

include wind speed ( $V$ ), wind direction ( $D$ ), temperature ( $T$ ) and turbulence intensity ( $I$ ). In Figure 1, we show the power curve plot and heat plot for the data from turbine R80790 as an example. Since no control/alarm records are provided, we first do rough filtering to separate the idle/controlled periods that can be indicated by the recorded variables, such as the pitch angle. Studies are conducted on every wind turbine during different time periods to show the wide applicability of DEAR. Only results regarding turbine R80790 is shown here. Details on the filtering and other studies can be seen in the supplementary file.

For this case study, we use a 45 days rolling window, as recommended in [Gneiting et al. \(2006\)](#), to estimate the up-to-date conditional mean and conditional density. This means that we use observations of approximately 45 days immediately before the first testing sample to do model inference. We choose the 30000th to 36500th points of year 2014 to conduct cross validation for input variable selection. The 36501th to 38500th points are chosen as testing dataset. Besides, wind speed and wind direction are always included for every three-dimensional input, as proposed by [Lee et al. \(2015\)](#). Moreover, wind speed is the most influential factor that affects conditional standard deviation. Evaluation based on RMSE has shown that considering wind speed as the only input when estimating  $\sigma(\cdot)$  is sufficient. Since  $\sigma(\cdot)$  is used to generate the homoscedastic residual ( $r_t$ ), we restrict the estimation of  $\sigma(\cdot)$  to be no smaller than the 0.5 percentile of the estimated range of  $\sigma(\cdot)$  to avoid computational problem.

**Table 1:** Performance comparison between different methods

Turbine	RMSE						CRPS	
	DEAR	AML	AMK	Binning	MSAR	Persistent	DEAR	AMK
R80790	<b>1.303</b>	2.757	2.895	3.185	6.589	5.160	<b>0.661</b>	3.437

We compare the performance of different methods in Table 1. It can be seen that AML slightly outperforms AMK for wind power curve because the local linear regression reduces bias. DEAR significantly outperforms AML, AMK and binning method by considering temporal dependence. Besides, DEAR outperforms other nonparametric regression and time

series analysis methods. For MSAR and persistent model, they focuses on wind power only and uses regime to capture different patterns. However, weather conditions are crucial for power curve. Ignoring weather conditions causes unsatisfying performance of these typical time series analysis methods.

To emphasize DEAR’s effectiveness on accounting for short-term temporal dependence, we compare DEAR with KDES in Table 2. At instant  $T$ , KDES use a forgetting factor  $\lambda$  that assign weight  $\lambda^{T-i}$  to the  $i$ th historical observation. KDES outperforms AML when a proper forgetting factor is used. Nevertheless, the performance of KDES is not as good as DEAR. When  $\lambda$  becomes smaller, KDES is more effective to capture short-term temporal dependence by assigning higher weights to more recent data. However, the RMSE in Table 2 is increasing when  $\lambda$  becomes smaller, which indicates bad performance. When  $\lambda$  becomes even smaller, KDES faces computation problems because of sparsity. Based on this analysis, it is reasonable to believe that KDES is more suitable for relatively long-term temporal dependence, such as system degradation. At the same time, DEAR outperforms KDES on short-term forecasting.

**Table 2:** Comparison between DEAR and KDES on Turbine R27890.

		RMSE			
DEAR	AML	KDES( $\lambda = 0.9995$ )	KDES( $\lambda = 0.999$ )	KDES( $\lambda = 0.998$ )	KDES( $\lambda = 0.995$ )
1.303	2.757	2.740	2.760	2.783	2.818

In the following, we use plots to intuitively explain DEAR’s performance. For DEAR’s conditional mean estimator, Figure 4 plots the point estimation of different models using wind speed as the horizontal axis and wind power as the vertical axis. We can see that the performance of DEAR is better than AMK especially on those areas when the observations have relatively large deviations from theoretical wind power curve.

Figure 5 illustrates DEAR’s conditional density estimation. The left panel is the confidence intervals constructed by DEAR and AMK shifted by the estimated conditional mean. The conditional mean residuals of DEAR and AMK are also shown. It can be seen that

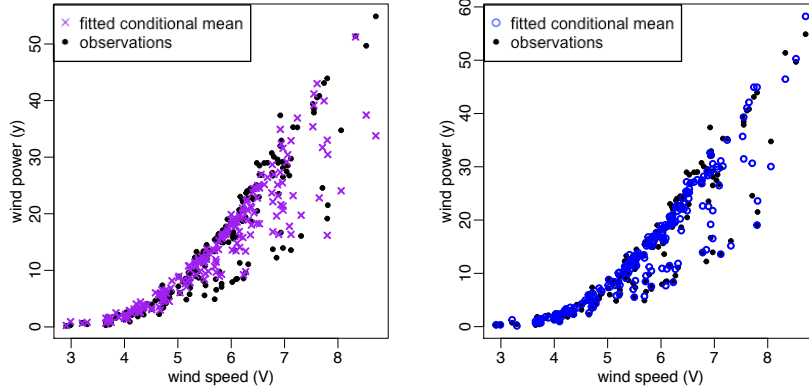


**Figure 4:** Conditional mean estimator illustration. Left panel: AMK; Right panel: DEAR.

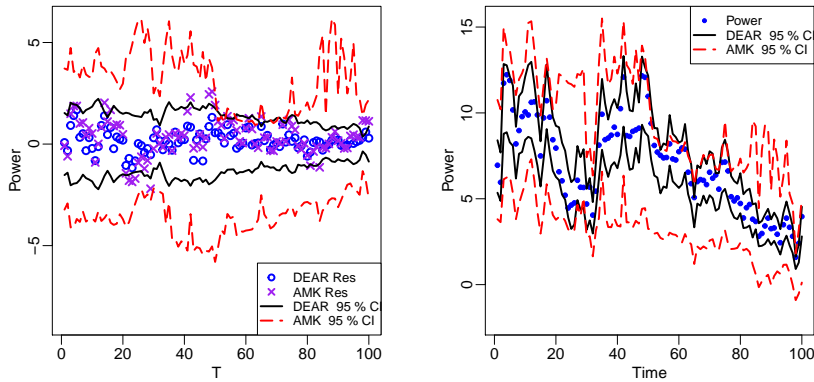


**Figure 5:** Conditional density estimator visualization for wind energy; Left panel: confidence interval normalized by estimated conditional mean; Right panel: Confidence interval of wind power output.

DEAR has both smaller residual and smaller confidence interval compared to AMK. The smaller residual of DEAR comes from the calibration of bias and autocorrelated error of the conditional mean. The smaller confidence interval comes from the calibration of bias of the conditional density. The CRPS value verifies that this smaller confidence interval is better. In the right panel, we plot the confidence intervals against the real values of power ( $Y$ ) are also shown. It can be seen that the confidence interval of DEAR moves better with the real values of  $Y$ , in a sense that it makes adjustments in response to the short-term data features. Moreover, since DEAR accounts for the autocorrelation, it provides different estimated mean and confidence interval at different instants even for the same weather input.

## 4.2 Case 2: Solar Power Curve Estimation

This dataset is from the Global Energy Forecasting Competition 2014 (GEFCom2014) (Hong et al., 2016). In this dataset, there are around 20000 hourly average records on solar power production as well as 12 weather condition variables from a solar power plant located in Australia. Some related weather conditions include surface pressure, relative humidity, wind speed, temperature and surface solar radiance. The aim is to estimate the distribution of solar power production given the weather variables. Besides the weather condition, we also consider one more input variable, time of the day, which has been proved to be effective on solar power estimation in literature such as Bacher et al. (2009). In this case study, we use the 1st to 10000th points to conduct cross validation to choose input variables. A rolling window of 6500 points is used for model inference. The 10001th to 12000th points are chosen as the testing dataset.

In this case, similarly as the the wind power case, we choose time of the day to estimate conditional standard deviation and restricted  $\sigma(\cdot)$  to be no smaller than the 0.5 percentile of the estimated range of  $\sigma(\cdot)$  to avoid computational problem. It can be seen from Table 3 that

**Table 3:** Performance comparison among different methods for solar power

RMSE					CRPS	
DEAR	AMK	Binning	MSAR	Persistent	DEAR	AMK
<b>6.603</b>	10.112	15.406	8.909	10.291	<b>0.304</b>	3.097

DEAR outperforms the other nonparametric or time series analysis methods regarding both RMSE and CRPS. Different from the wind power case, the solar power dataset has higher uncertainty, hence persistent model and MSAR performs better than the nonparametric regression models, i.e., AMK and binning methods. This is reasonable because the high uncertainty we observed is caused by the fact that the available covariates have weak explainability. As a result, nonparametric regressions that rely on the covariates provide relatively unsatisfying results. Time series models fit the data better by relying on the temporal-dependent relationship and the previous observations. Nevertheless, DEAR always performs

the best since it is able to include the effects of both available predictors and temporal dependence.

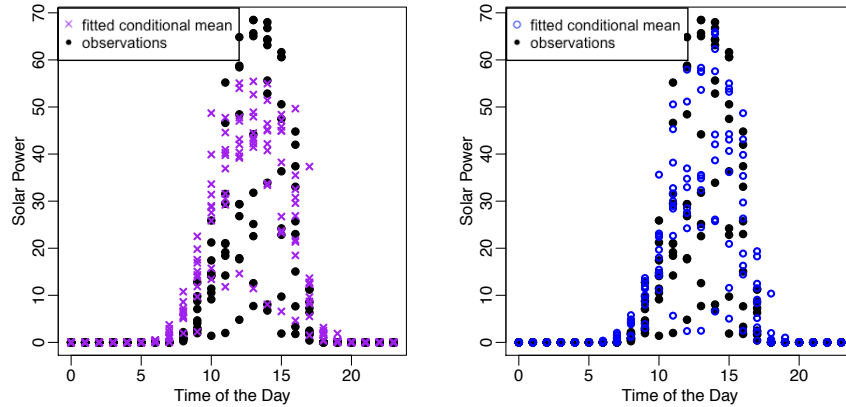


**Figure 6:** Conditional mean prediction for solar energy. Left panel: AMK; Right panel: DEAR.

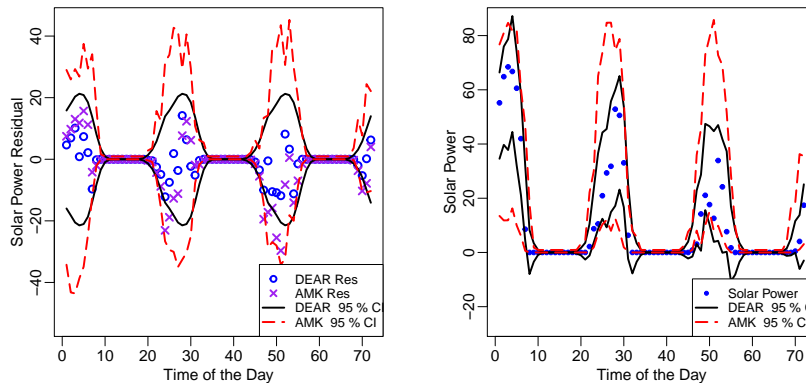


**Figure 7:** Conditional density estimator visualization for solar energy; Left panel: confidence interval normalized by estimated conditional mean; Right panel: Confidence interval of solar power output.

## 5 Conclusion

Power generation from renewable energy sources, such as wind and solar, has grown rapidly and become indispensable for energy security and global warming mitigation. Since the fluctuations of renewable energy generation are hard to be model by first principles, accurate power curve modeling using data driven methods is essential for RE's control strategies,

security of electrical grid and power trading etc. The data characteristics, unknown conditional distribution and highly interactive weather conditions, make conditional density estimation necessary. In this paper, we propose DEAR to take care of temporal dependence when doing conditional density estimation. In this way, our proposed method manages to account for all three data characteristics, which effectively improves both conditional mean and density estimators. Real-field case studies from wind and solar energy are used to show the effectiveness of DEAR compared to other existing methods. In the future, DEAR can be used to construct real time condition monitoring schemes for RE equipments. This can help to better understand the systems' operation status and respond to failure or suboptimal status as soon as possible. In addition, it is possible to construct model for larger systems, such as wind farms. In this case, intra-system interactions, such as wake effects among wind turbines, need to be further considered.

## References

- Ackermann, T. (2005). *Wind power in power systems*. John Wiley & Sons.
- Aho, J., Buckspan, A., Laks, J., Fleming, P., Jeong, Y., Dunne, F., Churchfield, M., Pao, L., and Johnson, K. (2012). A tutorial of wind turbine control for supporting grid frequency through active power control. In *American Control Conference (ACC), 2012*, pages 3120–3131. IEEE.
- Bacher, P., Madsen, H., and Nielsen, H. A. (2009). Online short-term solar power forecasting. *Solar Energy*, 83(10):1772–1783.
- Bessa, R. J., Miranda, V., Botterud, A., Wang, J., and Constantinescu, E. M. (2012). Time adaptive conditional kernel density estimation for wind power forecasting. *IEEE Transactions on Sustainable Energy*, 3(4):660–669.
- Blonbou, R. (2011). Very short-term wind power forecasting with neural networks and adaptive bayesian learning. *Renewable Energy*, 36(3):1118–1124.
- Cochran, J., Bird, L., Heeter, J., and Arent, D. (2012). Integrating variable renewable energy in electric power markets: Best practices from international experience. Technical report, National Renewable Energy Lab.(NREL), Golden, CO (United States).
- Ding, Y., Tang, J., and Huang, J. Z. (2015). Data analytics methods for wind energy applications. In *ASME Turbo Expo 2015: Turbine Technical Conference and Exposition*, pages V009T46A020–V009T46A020. American Society of Mechanical Engineers.
- Fusco, F. and Ringwood, J. V. (2010). Short-term wave forecasting for real-time control of wave energy converters. *IEEE Transactions on Sustainable Energy*.
- Gneiting, T., Larson, K., Westrick, K., Genton, M. G., and Aldrich, E. (2006). Calibrated probabilistic forecasting at the stateline wind energy center: The regime-switching space-time method. *Journal of the American Statistical Association*, 101(475):968–979.

- Golestaneh, F., Pinson, P., and Gooi, H. B. (2016). Very short-term nonparametric probabilistic forecasting of renewable energy generation - With application to solar energy. *IEEE Transactions on Power Systems*, 31(5):3850–3863.
- Hastie, T. and Loader, C. (1993). Local regression: Automatic kernel carpentry. *Statistical Science*, pages 120–129.
- Hong, T., Pinson, P., Fan, S., Zareipour, H., Troccoli, A., and Hyndman, R. J. (2016). Probabilistic energy forecasting: Global Energy Forecasting Competition 2014 and beyond. *International Journal of Forecasting*, 32(3):896–913.
- Hyndman, R. J., Bashtannyk, D. M., and Grunwald, G. K. (1996). Estimating and visualizing conditional densities. *Journal of Computational and Graphical Statistics*, 5(4):315–336.
- IRENA (2019). Solutions to integrate high shares of variable renewable energy (report to the g20 energy transitions working group (etwg)). Technical report, International Renewable Energy Agency, Abu Dhabi.
- Jeon, J. and Taylor, J. W. (2012). Using conditional kernel density estimation for wind power density forecasting. *Journal of the American Statistical Association*, 107(497):66–79.
- Jeon, J. and Taylor, J. W. (2016). Short-term density forecasting of wave energy using ARMA-GARCH models and kernel density estimation. *International Journal of Forecasting*, 32(3):991–1004.
- Lauret, P., Voyant, C., Soubdhan, T., David, M., and Poggi, P. (2015). A benchmarking of machine learning techniques for solar radiation forecasting in an insular context. *Solar Energy*, 112:446–457.
- Lave, M., Kleissl, J., and Stein, J. S. (2012). A wavelet-based variability model (wvm) for solar pv power plants. *IEEE Transactions on Sustainable Energy*, 4(2):501–509.
- Lee, G., Ding, Y., Genton, M. G., and Xie, L. (2015). Power curve estimation with multivariate environmental factors for inland and offshore wind farms. *Journal of the American Statistical Association*, 110(509):56–67.
- Lei, M., Shiyang, L., Chuanwen, J., Hongling, L., and Yan, Z. (2009). A review on the forecasting of wind speed and generated power. *Renewable and Sustainable Energy Reviews*, 13(4):915–920.
- Lydia, M., Kumar, S. S., Selvakumar, A. I., and Kumar, G. E. P. (2014). A comprehensive review on wind turbine power curve modeling techniques. *Renewable and Sustainable Energy Reviews*, 30:452–460.
- Ma, J., Makarov, Y. V., Loutan, C., and Xie, Z. (2011). Impact of wind and solar generation on the California ISO’s intra-hour balancing needs. In *IEEE Power and Energy Society General Meeting*.
- Pinson, P., Chevallier, C., and Kariniotakis, G. N. (2007). Trading wind generation from short-term probabilistic forecasts of wind power. *IEEE Transactions on Power Systems*, 22(3):1148–1156.
- Pinson, P. and Madsen, H. (2012). Adaptive modelling and forecasting of offshore wind power fluctuations with markov-switching autoregressive models. *Journal of Forecasting*, 31(4):281–313.
- Pinson, P., Reikard, G., and Bidlot, J.-R. (2012). Probabilistic forecasting of the wave energy flux. *Applied energy*, 93:364–370.
- Rosenblatt, M. (1969). Conditional probability density and regression estimators. *Multivariate analysis II*, 25:31.



- Ruppert, D., Sheather, S. J., and Wand, M. P. (1995). An effective bandwidth selector for local least squares regression. *Journal of the American Statistical Association*, 90(432):1257–1270.
- Sanchez, I. (2006). Short-term prediction of wind energy production. *International Journal of Forecasting*, 22(1):43–56.
- Sheather, S. J. and Jones, M. C. (1991). A reliable data-based bandwidth selection method for kernel density estimation. *Journal of the Royal Statistical Society. Series B (Methodological)*, pages 683–690.
- Silverman, B. W. (1986). *Density estimation for statistics and data analysis*, volume 26. CRC press.
- Sohoni, V., Gupta, S., and Nema, R. (2016). A critical review on wind turbine power curve modelling techniques and their applications in wind based energy systems. *Journal of Energy*, 2016.
- Taylor, C. C. (2008). Automatic bandwidth selection for circular density estimation. *Computational Statistics & Data Analysis*, 52(7):3493–3500.
- Taylor, J. and Einbeck, J. (2013). Challenging the curse of dimensionality in multivariate local linear regression. *Computational Statistics*, 28(3):955–976.
- Wand, M. P. and Jones, M. C. (1994). Multivariate plug-in bandwidth selection. *Computational Statistics*, 9(2):97–116.
- Xiao, Z., Linton, O. B., Carroll, R. J., and Mammen, E. (2003). More efficient local polynomial estimation in nonparametric regression with autocorrelated errors. *Journal of the American Statistical Association*, 98(464):980–992.
- Yuan, Y., Chen, N., and Zhou, S. (2017). Modeling regression quantile process using monotone b-splines. *Technometrics*, 59(3):338–350.
- Zhang, J., Zhao, L., Deng, S., Xu, W., and Zhang, Y. (2017). A critical review of the models used to estimate solar radiation. *Renewable and Sustainable Energy Reviews*, 70:314–329.

# Supplementary Material to “Conditional Kernel Density Estimation Considering Autocorrelation for Renewable Energy Probabilistic Modeling”

Yuchen SHI and Nan CHEN

Department of Industrial Systems Engineering and Management  
National University of Singapore  
Singapore

## Appendix A The Optimal Direct Plug-in Bandwidths

The optimal bandwidth for  $\tilde{m}(\cdot)$  when using local linear regression can be found as:

$$h_j \simeq \left[ R(K) \int \sqrt{\sigma(x)} dx / \{ T\mu_2(K)^2 \int m^2(x)^2 f(x) dx \} \right]^{1/5},$$

where  $\mu_l(L) = \int u^l L(u) du$  denotes the  $l$ th moment with respect to distribution  $L$  and  $R(L) = \int L(u)^2 du$  denotes the square integral of  $L$ .  $K$  denotes for the kernel function.  $f$  denotes the density function of  $x$ .

The optimal bandwidth for density estimator of residual  $\tilde{m}(\cdot)$  when using traditional kernel method and is:

$$h \simeq [R(K) / \{ \mu^4(K) R(g'') \}]^{1/5} n^{-1/5}.$$

Here  $g$  denotes the density function of  $r$ . The unknown integrals in the optimal bandwidth can be substituted by their corresponding estimators to obtain the optimal plug-in bandwidths.

## Appendix B Local Linear Regression

For notation simplicity, we define

$$\mathbf{y} = \begin{pmatrix} Y_1 \\ \vdots \\ Y_T \end{pmatrix}, \mathbf{x} = \begin{pmatrix} 1 & (\mathbf{X} - \mathbf{X}_1)' \\ & \vdots \\ 1 & (\mathbf{X} - \mathbf{X}_T)' \end{pmatrix}, \mathbf{W} = \text{diag}([\mathcal{K}(\|\mathbf{X} - \mathbf{X}_1\|; \mathbf{h}_{\mathbf{X}}), \dots, \mathcal{K}(\|\mathbf{X} - \mathbf{X}_T\|; \mathbf{h}_{\mathbf{X}})]).$$

Here  $\text{diag}([v_1, v_2, \dots, v_n])$  denotes a  $n \times n$  diagonal matrix with the  $i$ th diagonal element being  $v_i$ . When the data are *i.i.d.*, an estimator of  $m(\cdot)$  obtained by local linear regression can be written as:

$$\tilde{m}(\mathbf{X}) = \mathbf{e}'_1 (\mathbf{x}' \mathbf{W} \mathbf{x})^{-1} \mathbf{x}' \mathbf{W} \mathbf{y}, \quad (1)$$

where  $\mathbf{e}_1$  is a  $(d+1) \times 1$  vector with 1 in the first element and zeros elsewhere. Based on  $Z_t = [Y_t - \tilde{m}(\mathbf{X}_t)]^2$  for  $t = 1, \dots, T$ , define

$$\mathbf{W}_\sigma = \text{diag}([\mathcal{K}(\|\mathbf{X} - \mathbf{X}_1\|; \mathbf{h}'_{\mathbf{X}}), \dots, \mathcal{K}(\|\mathbf{X} - \mathbf{X}_T\|; \mathbf{h}'_{\mathbf{X}})]),$$

where the bandwidth  $\mathbf{h}'_{\mathbf{X}}$  are chosen adaptively by  $\mathcal{G}_T := \{(\mathbf{X}_t, Z_t), t = 1, \dots, T\}$ . Therefore, the local linear kernel estimation of the variance function becomes

$$\tilde{\sigma}(\mathbf{X}) = \sqrt{\mathbf{e}'_1 (\mathbf{x}' \mathbf{W}_\sigma \mathbf{x})^{-1} \mathbf{x}' \mathbf{W} \mathbf{z}}, \quad (2)$$

where  $\mathbf{z} = [Z_1, \dots, Z_T]'$ .

# Appendix C Additional Numerical Results: The La Haute Borne Case Study

Since no control/alarm records are provided in this dataset, we first do rough filtering to separate the variabilities that can be indicated by the recorded variables using the following rules: (1) Remove the points with non-positive power output, which indicate idle state. (2) Remove points next to idle state, which are at startup/shutting down state. (3) Remove points whose pitch angles are higher than  $15^\circ$  or higher than  $1^\circ$  when wind speed is lower than 8 m/s, which indicate pitch control. The wind power data before and after filtering can be seen in Figure C.1.

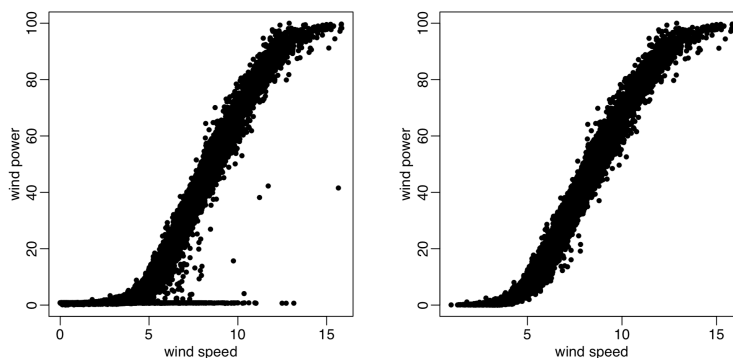


**Figure C.1:** R80721 conditional density estimation visualization; Left panel: confidence interval of wind power’s conditional density estimator in the order of time; Right panel: Confidence interval of wind power’s conditional density estimator in the order of wind speed.

Additional to the study conducted on turbine R80790, we conducted three more studies, with details listed in Table 1. The cross validation dataset is used for input variable selection. These three studies are conducted using data from year 2013. We deliberately choose different time periods for different studies to show the wide applicability of DEAR. The comparison results of the extra studies can be seen in Table 2. The visualization of the extra studies can be seen in Figure C.2 to C.7.

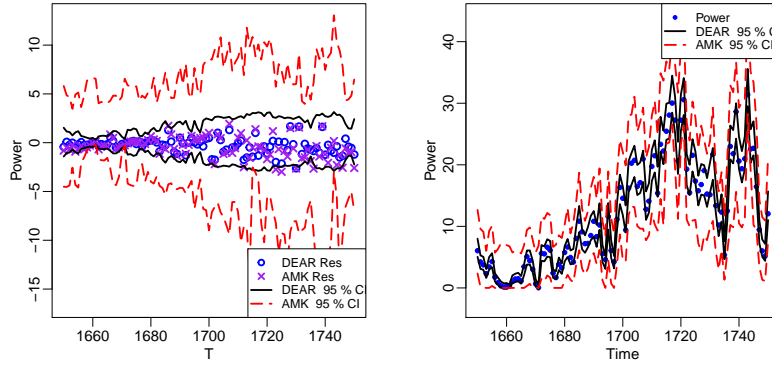


**Figure C.2:** R80711 conditional density estimation visualization; Left panel: confidence interval in the order of time; Right panel: Confidence interval of wind power's conditional density estimator in the order of wind speed.

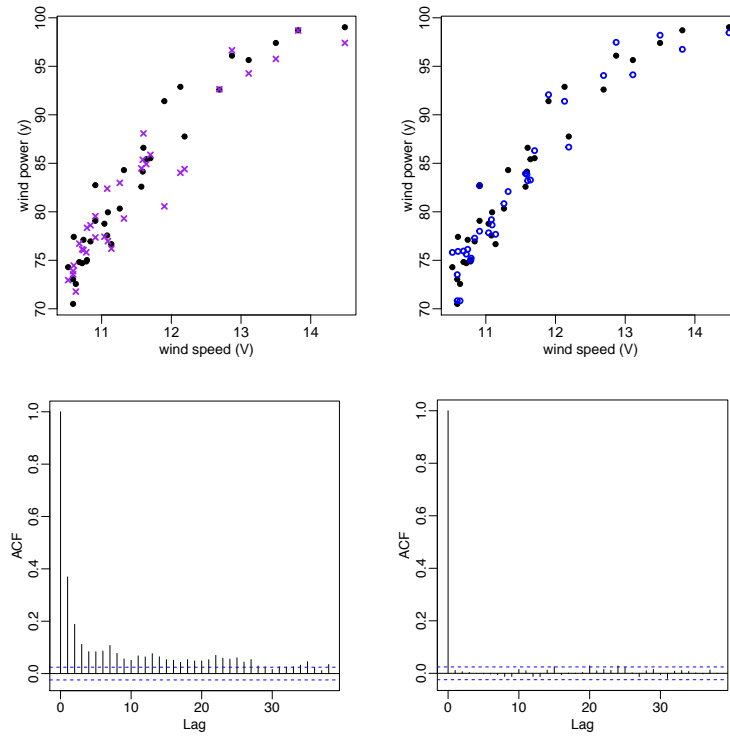


**Figure C.3:** R80711 conditional mean estimation visualization; Left panel: AMK estimation; Right panel: DEAR estimation.

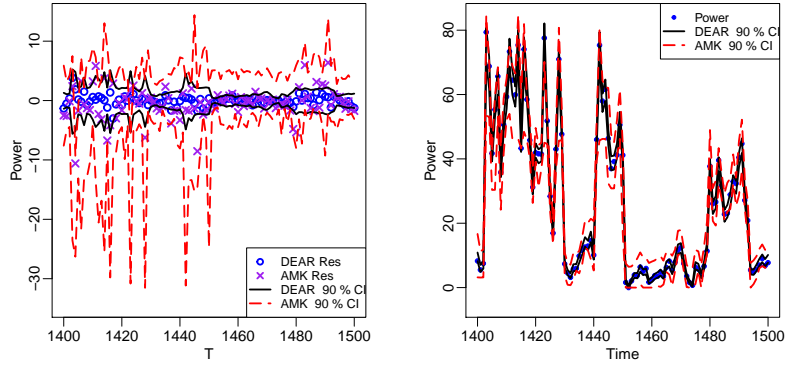


**Figure C.4:** R80721 conditional density estimation visualization; Left panel: confidence interval of wind power's conditional density estimator in the order of time; Right panel: Confidence interval of wind power's conditional density estimator in the order of wind speed.

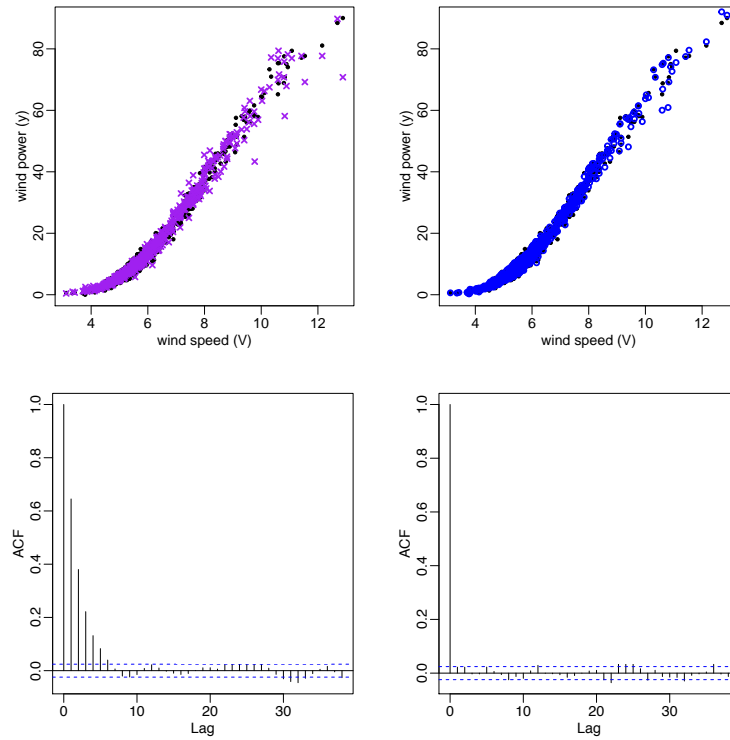


**Figure C.5:** R80721 conditional mean estimation visualization; Left panel: AMK estimation; Right panel: DEAR estimation.

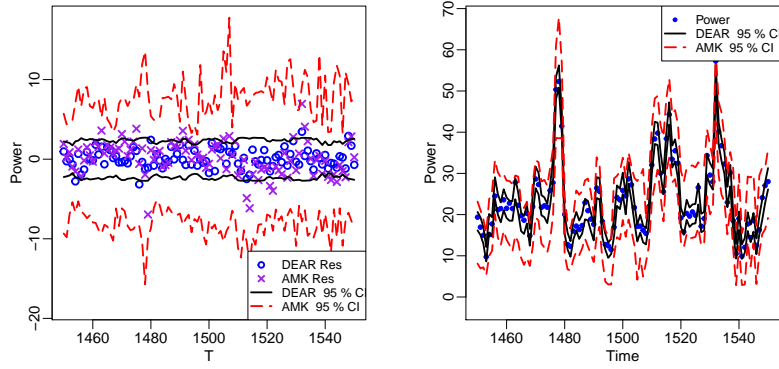


**Figure C.6:** R80736 conditional density estimation visualization; Left panel: confidence interval of wind power's conditional density estimator in the order of time; Right panel: Confidence interval of wind power's conditional density estimator in the order of wind speed.

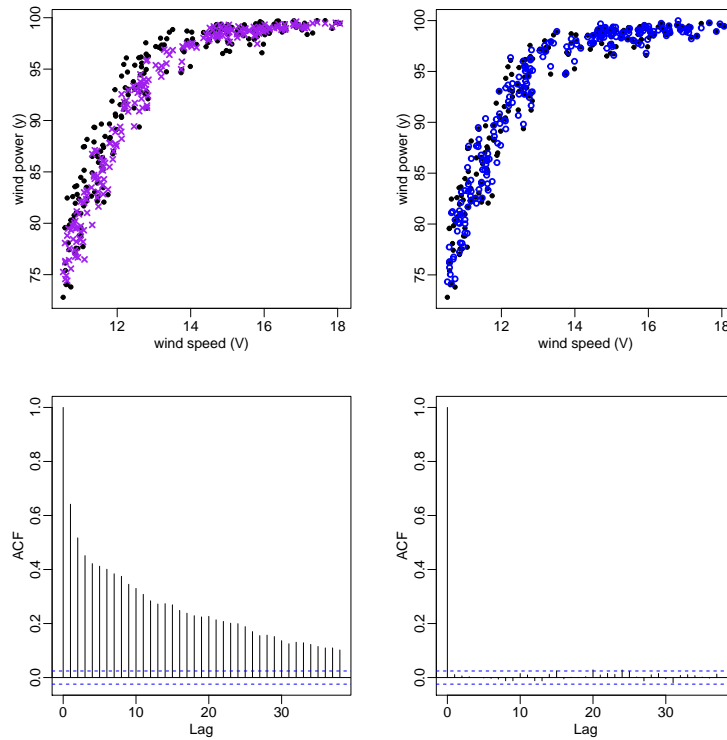


**Figure C.7:** R80736 conditional mean estimation visualization; Left panel: AMK estimation; Right panel: DEAR estimation.

**Table 1:** Experiments

Case	Cross Validation	Testing	AMK Variables	AML Variables
R80711	1:16500	16501:18500	V D T I	V D T I
R80721	1:16500	16501:18500	V D T I	V D T I
R80736	20001:36500	36501:38500	V D I	V D T I

**Table 2:** Performance comparison between different methods

Turbine	RMSE						CRPS	
	DEAR	AML	AMK	Binning	MSAR	Persistent	DEAR	AMK
R80711	<b>0.999</b>	1.932	1.958	2.009	6.711	5.749	<b>0.530</b>	1.557
R80721	<b>0.801</b>	1.796	1.787	2.137	7.287	7.512	<b>0.593</b>	1.058
R80736	<b>1.023</b>	1.895	1.938	1.783	9.843	6.037	<b>0.728</b>	1.558

## Appendix D DEAR Algorithm



---

**Algorithm 1** Conditional Kernel Density Estimation Considering Autocorrelation
 

---

**Input:**  $\mathcal{F}_T = \{(\mathbf{X}_i, Y_i), i = 1, \dots, T\}$ ;  $T$ : rolling window;  $\mathcal{K}$ : kernel functions.

**Inference Procedure:**

- 1: For  $t = 1, \dots, T$ , obtain initial estimates of  $m(\cdot)$  and  $\sigma(\cdot)$ .
  - (1) Calculate the bandwidth of input variables ( $\tilde{\mathbf{h}}_{\mathbf{X}}$ ) and the conditional mean  $\tilde{m}(\mathbf{X}_t)$  using  $\mathcal{F}_T = \{(\mathbf{X}_t, Y_t), t = 1, \dots, T\}$ .
  - (2) Calculate the bandwidth of input variables ( $\tilde{\mathbf{h}}'_{\mathbf{X}}$ ) and the conditional standard deviation  $\tilde{\sigma}(\mathbf{X}_t)$  using  $\mathcal{G}_T = \{(\mathbf{X}_t, Z_t), t = 1, \dots, T\}$ .
- 2: Initialize  $\hat{m}(\mathbf{X}_t) = \tilde{m}(\mathbf{X}_t)$  and  $\hat{\sigma}(\mathbf{X}_t) = \tilde{\sigma}(\mathbf{X}_t)$ .
- 3: Calculate  $\tilde{u}_t = [Y_t - \hat{m}(\mathbf{X}_t)]/\hat{\sigma}(\mathbf{X}_t)$ .
- 4: While the termination condition is not satisfied, do:
  - (1) Obtain  $p$  and  $\hat{a}_1, \dots, \hat{a}_p$  using  $\tilde{u}_t$ .
  - (2) Calibrate  $Y_t$  to  $\tilde{Y}_t$  and obtain the calibrated observations  $\tilde{\mathcal{F}}_T = \{(\mathbf{X}_t, \tilde{Y}_t), t = 1, \dots, T\}$ .
  - (3) Re-calculate  $\hat{\mathbf{h}}_{\mathbf{X}}$  and  $\hat{m}(\mathbf{X}_t)$  using  $\tilde{\mathcal{F}}_T$ .
  - (4) Re-calculate  $\hat{\mathbf{h}}'_{\mathbf{X}}$  and  $\hat{\sigma}(\mathbf{X}_t)$  using  $\tilde{\mathcal{G}}_T = \{(\mathbf{X}_t, \tilde{Z}_t), t = 1, \dots, T\}$ .
  - (5) Re-calculate  $\tilde{u}_t$ .
  - (6) Calculate  $r_t$  and check the autocorrelation among  $r_t$ . Terminate the inference procedure if  $r_t$  pass the Box-Ljung test.
- 5: Record  $\hat{\mathcal{U}}_T = \{\hat{u}_t = \hat{\sigma}(\mathbf{X}_t)^{-1}[Y_t - \hat{m}(\mathbf{X}_t)], t = 1, \dots, T\}$ .
- 6: Record  $\hat{\mathcal{F}}_T = \{(\mathbf{X}_t, \hat{Y}_t), t = 1, \dots, T\}$ , where  $\hat{Y}_t = Y_t - \hat{\sigma}(\mathbf{X}_t) \sum_{\tau=1}^p \hat{a}_\tau \hat{u}_{t-\tau}$ .
- 7: Record  $\mathcal{R}_T = \{r_t = (Y_t - \hat{\mu}_{t|t-1})/\hat{\sigma}(\mathbf{X}_t), t = 1, \dots, T\}$ .
- 8: Calculate  $\hat{h}_{\epsilon,t}$  using  $\mathcal{R}_T$ .

**Prediction Procedure:**

- 9: For the next instant  $T + 1$ :
    - (1) Estimate the conditional mean  $\hat{\mu}_{T+1|T}$  using  $\hat{\mathcal{F}}_T$ .
    - (2) Given any  $Y_{T+1}$  of interest, estimate the conditional density  $\hat{f}(Y_{T+1}|\mathbf{X}_{T+1}, \mathcal{F}_T)$
    - (3) Calculate  $\hat{Y}_{T+1}$ ,  $\hat{u}_{T+1}$ , and  $r_{T+1}$ ; Update  $\hat{\mathcal{F}}_T$ ,  $\hat{\mathcal{U}}_T$  and  $\mathcal{R}_T$  using the window  $\{2, \dots, T + 1\}$ .
-